# The Last Glacial Termination

G. H. Denton,[1] R. F. Anderson,[2,3]* J. R. Toggweiler,[4] R. L. Edwards,[5]
J. M. Schaefer,[2,3] A. E. Putnam[1]

A major puzzle of paleoclimatology is why, after a long interval of cooling climate, each late Quaternary ice age ended with a relatively short warming leg called a termination. We here offer a comprehensive hypothesis of how Earth emerged from the last global ice age. A prerequisite was the growth of very large Northern Hemisphere ice sheets, whose subsequent collapse created stadial conditions that disrupted global patterns of ocean and atmospheric circulation. The Southern Hemisphere westerlies shifted poleward during each northern stadial, producing pulses of ocean upwelling and warming that together accounted for much of the termination in the Southern Ocean and Antarctica. Rising atmospheric $CO_2$ during southern upwelling pulses augmented warming during the last termination in both polar hemispheres.

At the peak of the last ice age, expansive ice sheets covered large areas of the Northern Hemisphere (NH) (Fig. 1). The reduction of this continental ice to about its present volume represents one of the largest and most rapid natural climate changes in Earth's recent history. As a consequence, identifying the conditions and processes that triggered this deglaciation has been a major objective of paleoclimate research [supporting online material (SOM)].

The last deglaciation was part of a recurring pattern of ice-sheet growth and decay (Fig. 2). Late Quaternary glacial cycles varied between 80,000 and 120,000 years in length, with an average recurrence interval of about 100,000 years. These cycles have asymmetric signatures, featuring a long cooling interval marked by an oscillating buildup of ice sheets to maximum volume followed by a relatively short warming period. During deglaciations, huge NH ice sheets (Fig. 1) melted away, sea level rose about 120 m (Fig. 2), atmospheric $CO_2$ increased by about 100 parts per million by volume (ppmv) (Fig. 3K), and interglacial climate emerged across the planet. The relatively rapid transitions from glacial to interglacial conditions have been dubbed terminations (*1*). The last ice recession began in the NH about 20,000 years ago (*2*, *3*), and by 7000 years ago all that was left of the great Laurentide Ice Sheet that had covered northern North America was a small ice cap on Baffin Island (*4*). In Antarctica and the Southern Ocean the last termination began about 18,000 years ago, with interglacial temperature attained close to 11,000 years ago (Fig. 3J).

[1]Department of Earth Sciences and Climate Change Institute, Bryand Global Sciences Center, University of Maine, Orono, ME 04469, USA. [2]Lamont-Doherty Earth Observatory of Columbia University, Post Office Box 1000, Palisades, NY 10964, USA. [3]Department of Earth and Environmental Sciences, Columbia University, New York, NY 10025, USA. [4]Geophysical Fluid Dynamics Laboratory, National Oceanic and Atmospheric Administration, Princeton, NJ 08542, USA. [5]Department of Geology and Geophysics, University of Minnesota, Minneapolis, MN 55455, USA.

*To whom correspondence should be addressed. E-mail: boba@ldeo.columbia.edu

The retreat of the huge NH ice sheets during the last termination sent bursts of melt water and icebergs into the northern North Atlantic Ocean, where they initiated thousand-year-long intervals of cold stadial climate. Here, we describe a sequence of global environmental changes initiated by those bursts, including the warming of Antarctica. Interhemispheric teleconnections, reinforced by rising atmospheric $CO_2$, allowed Earth to emerge from the last ice age.

### NH Summer Insolation

Based on the proposition that marginal melting dominates mass balance, Milankovitch (*5*) postulated that variations in summer insolation at high latitudes caused waxing and waning of northern ice sheets. That orbital oscillations strongly influenced northern ice sheets is supported by the connection between ice-volume change and the concomitant variations of summer insolation (Fig. 2B) (*6*). Well-dated paleoclimate proxies from Chinese caves (*7*), the Dome Fuji ice core in Antarctica (*8*), and marine sediment cores (*9*) indicate that rising northern summer insolation accompanied terminations. However, increasing northern summer insolation also occurred elsewhere in the glacial record where no terminations took place (Fig. 2B). Moreover, full terminations occurred both when the amplitude of summer insolation change was high [e.g., ter-

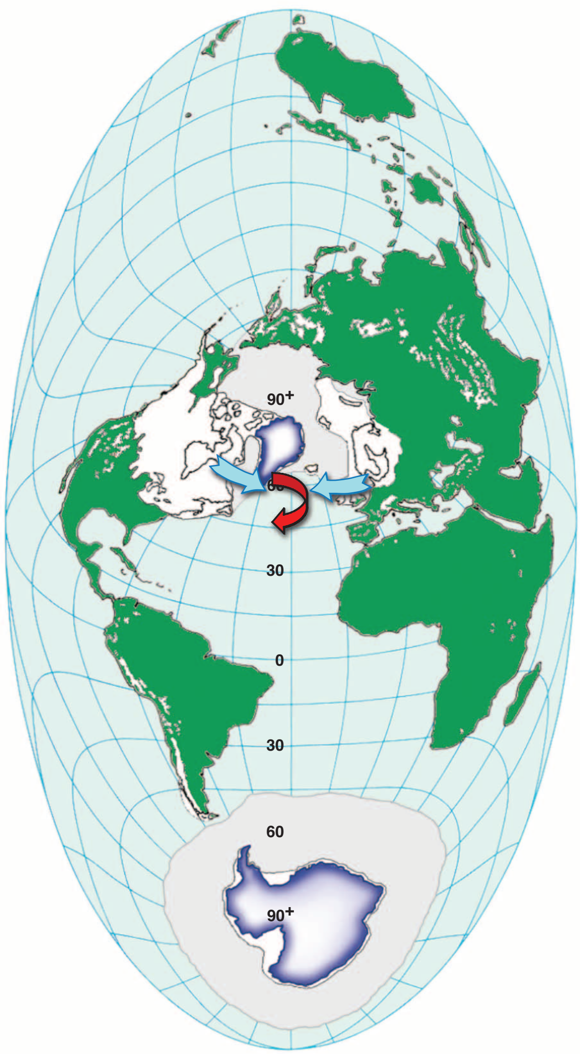


**Fig. 1.** Representative changes in the volume of continental ice throughout the Late Pleistocene. Global map showing the schematic spatial extent of continental ice sheets (white shading) at the LGM (*61*, *62*). Two large ice sheets (outlined in blue) survived the last termination. One is in Greenland and the other in Antarctica. This map projection emphasizes the proximity of the Laurentide and European ice sheets to areas of deepwater formation in the North Atlantic Ocean (red arrow, indicating a general region without implying a specific mechanism or site of deepwater formation). Blue arrows indicate the supply of freshwater and icebergs. On the Southern Ocean, gray shading indicates maximum extent of winter sea ice (*63*).

mination 2 (T2) and T4 (Fig. 2B)] and when it was low [e.g., T1 and T3 (Fig. 2B)]. Therefore, rising insolation alone is insufficient to explain terminations.

## Large Ice Sheets

Terminations invariably began when ice sheets were at or close to their greatest area and volume. This striking situation affords an important clue in deciphering their cause(s). Specifically, as described below, a large volume of NH ice represents the essential initial condition for a termination [supporting online material (SOM)]. Raymo (*10*) pointed out that terminations ending in full interglacial climate occurred only after ice sheets achieved what she defined as "excess" volume at glacial maxima, derived from benthic oxygen-isotope ratios in deep-sea cores (Fig. 2B). This "excess" ice must have been tied up in NH ice sheets because the Antarctic sheet contributed only 14 m or less to the total drop of sea level of about 120 m at the last glacial maximum (LGM) (*11*). Figure 1 shows that most northern sheets, of which the Laurentide was by far the largest, were arrayed around the critical North Atlantic deepwater downwelling sites. When at their largest, these sheets expanded across continental shelves, had maximum isostatic depression beneath them, and were drained seaward by ice streams. Ice-sheet sectors with such marine-based configurations were prone to unstable collapse into the adjacent ocean (SOM). Thus, the importance of Raymo's "excess" ice was that it provided the necessary volume in seaward-draining ice systems to produce a collapse into the North Atlantic that was massive and long enough to jump-start a termination via oceanic and atmospheric teleconnections with the Southern Hemisphere (SH), as described below.

Ice drainage systems that emptied into the North Atlantic produced copious quantities of icebergs and meltwater that affected northern overturning circulation [e.g., (*12*, *13*)]. Heinrich (*14*) discovered six distinctive deposits of ice-rafted lithic fragments dating to the last glacial cycle in deep-sea cores collected in the ice-rafting zone centered at ~50°N in the North Atlantic. Layers of detrital dolomitic carbonate, which dominate these deposits, can be traced to Hudson Strait. These carbonate layers record massive outbursts of icebergs that are a testament to episodes of Laurentide ice collapse. In addition to Canadian-sourced detrital carbonate, many of the lithic deposits in the North Atlantic ice-rafting zone contain important contributions from Greenland and European ice sheets (*15*), indicating the significance of these sources as well. The last of these massive outbursts of icebergs is termed Heinrich 1 and occurred near the onset of the last termination. In addition, summer melting during retreat of northern sheets injected fresh water into the North Atlantic. As a prominent example, Toucanne *et al.* (*3*) documented a massive discharge of melt water emanating from margins of European ice sheets through the Channel River between England and France into the North Atlantic early in the last termination, beginning about 20,000 years ago and reaching a maximum between 18,300 and 17,000 years ago. Abrupt expansion of polar planktonic foraminifera shortly before 18,000 years ago accompanied this meltwater pulse (*16*).

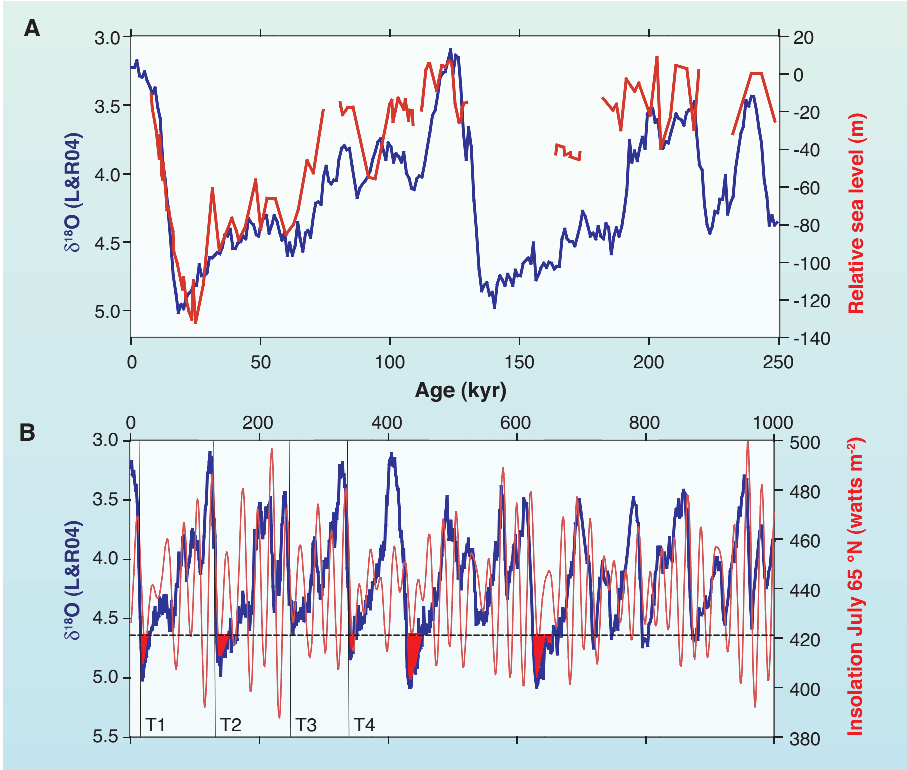


**Fig. 2.** (**A**) Two proxy records related to global ice volume during the past 250,000 years. The stacked record of the oxygen isotopic composition of benthic foraminifera recovered from 57 deep-sea cores [blue (*9*)] is influenced primarily by global ice volume but also secondarily by changes in the temperature of the deep ocean. Oxygen isotopes are plotted on a reverse scale, such that more-positive values (down) reflect greater volumes of continental ice. Changes in sea level relative to modern conditions (red), which are controlled by the amount of water locked up in continental ice, are estimated by uranium-thorium dating of corals that lived at a known depth (*64*). Before the last glacial cycle, the coral record is limited to high sea levels, but the record is sufficient to illustrate the robust relationship between sea level and the oxygen-isotope signal, which extends back much further in time. (**B**) The stacked oxygen-isotopic record from benthic foraminifera [blue (*9*)] is compared against July insolation at 65°N [red (*65*)] over the past 1,000,000 years. Periods of maximum global ice volume just before major terminations (shaded in red) are referred to in the text as excess ice (*10*). The level beyond which the oxygen-isotope record is shaded is intended to emphasize the point that terminations occur when continental ice volume is at or near its maximum and not to imply that a specific oxygen isotope value is required for a termination to occur. The extended Asian Monsoon record of Cheng *et al.* (*7*) supports the chronology and relationships illustrated here. Terminations 1 to 4, referred to in the text, are identified by vertical black lines.

During the last termination, such outbursts of meltwater and icebergs produced the Heinrich 1 and Younger Dryas stadials in the North Atlantic region by curtailing northern overturning circulation. In the case of Heinrich stadial 1 [HS1, as defined by (*17*), which is equivalent to the Mystery Interval of Denton *et al.* (*18*)], reduced overturning (Fig. 3F) was initiated and maintained by fresh water supplied by ice melt (*3*) and surges (*13*). Figure 3 illustrates the resulting situation south of the main ice-rafting zone in the subtropical northeast Atlantic near the Iberian Peninsula. There, ice rafting occurred in two pulses during HS1 (Fig. 3D) (*19*). A substantial drop in sea surface temperature (SST) and the expansion of polar planktonic foraminifera preceded the maximum ice-rafting spike (*16*). SST remained low between about 17,800 and 15,000 years ago during HS1 (Fig. 3E). Thus, HS1 featured widespread melt and collapse of Laurentide and European ice, along with cold SST and reduced overturning circulation in the North Atlantic. Figure 3 illustrates that the Younger Dryas stadial (YDS) was in many ways a replicate of HS1.

## Sea Ice and Seasonality

Proxy records show that an important consequence of weakened overturning circulation, combined with fresh water–induced stratification, was an expansion of winter sea ice that introduced a highly seasonal climate in the North Atlantic region (*20*–*23*), a result replicated in a model experiment (*24*). Such seasonality arose during stadials because the spread of winter sea ice created Siberian-like conditions, dominated by large temperature swings between winter and summer, in lands adjacent to and downwind of the North Atlantic. For example, mean annual temperatures in Greenland and northern Europe dropped 12° to 17°C below today's values in the YDS (*22*, *25*), partitioned into a 22° to 28°C shift in winter and a 3° to 6°C shift in summer (*20*–*22*). A similar seasonal difference marked northern Europe in HS1 (*23*).

Model results suggest that the expansion of sea ice across the northern North Atlantic, particularly in winter, was the key factor in spreading the impacts of the millennial-scale cold events quickly and efficiently throughout the NH and into the tropics. Chiang and Bitz (*24*) showed that the Intertropical Convergence Zone (ITCZ) in all ocean basins shifted away from the hemisphere with an imposed increased ice cover anomaly such as that on the North Atlantic during the YDS and HS1. Their findings are supported by the observation that the ITCZ and Trade Winds over South America (*26*, *27*) and across the tropical Pacific (*28*, *29*) varied during the last glacial period with a distinct pattern similar to stadial-interstadial switches in the North Atlantic, as well as by the observation that the Atlantic sector of the ITCZ was pushed south so much during HS1 that it rained in Brazil in areas normally arid (*30*). Weakening of the Asian monsoon during the YDS and HS1 (Fig. 3B) coincided with increased precipitation in Indonesia (*31*) and in northern Australia (*32*) as the ITCZ shifted southward. Barnett *et al*. (*33*) linked weakened Asian monsoons to cold and long Asian winters, such as might be imposed in the northern tier of the hemisphere, including Eurasia, as a consequence of a winter sea-ice cover on the northern North Atlantic. Evidence for changes in precipitation during North Atlantic stadials has been found throughout tropical Africa and extending to the southern tip of the continent (*34*). The impact of these events extended well into the SH.

## North-South Connections

Full-glacial conditions persisted in Antarctica until about 18 ka (Fig. 3J). The subsequent termination featured two warming pulses separated by the Antarctic Cold Reversal (ACR) (Fig. 3J). Similar features characterized the termination at SH middle latitudes. As atmospheric summer temperature rose about 6°C in the Chilean Lake District (Fig. 3H), Andean glaciers underwent considerable recession; for the first time in more than 50,000 years, a rainforest invaded the lowland (*35*). On both sides of the Pacific Ocean, mid-latitude SST rose in two steps by a total of more than 5°C (Fig. 3G) (*36*–*40*).

The first southern warming pulse coincided with HS1 and the second with the YDS (yellow bands in Fig. 3). Within each of these cold NH stadials, the north featured a slow down or cessation of North Atlantic overturning (Fig. 3F) accompanied by the spread of winter sea ice and cold ocean temperatures (Fig. 3E), with concomitant weakening of the Asian monsoon (Fig. 3B) and a southward shift of the ITCZ. In contrast, the SH featured increasing upwelling in the Southern Ocean (Fig. 3I) accompanied by a rise in atmospheric $CO_2$ (Fig. 3K) along with rapidly warming ocean temperatures (Fig. 3G). The behavior between the hemispheres was also opposite in the interval between the NH stadials. In the northern Bølling-Allerød, North Atlantic overturning circulation resumed (Fig. 3F), forcing a retreat of winter sea ice and hence a rapid

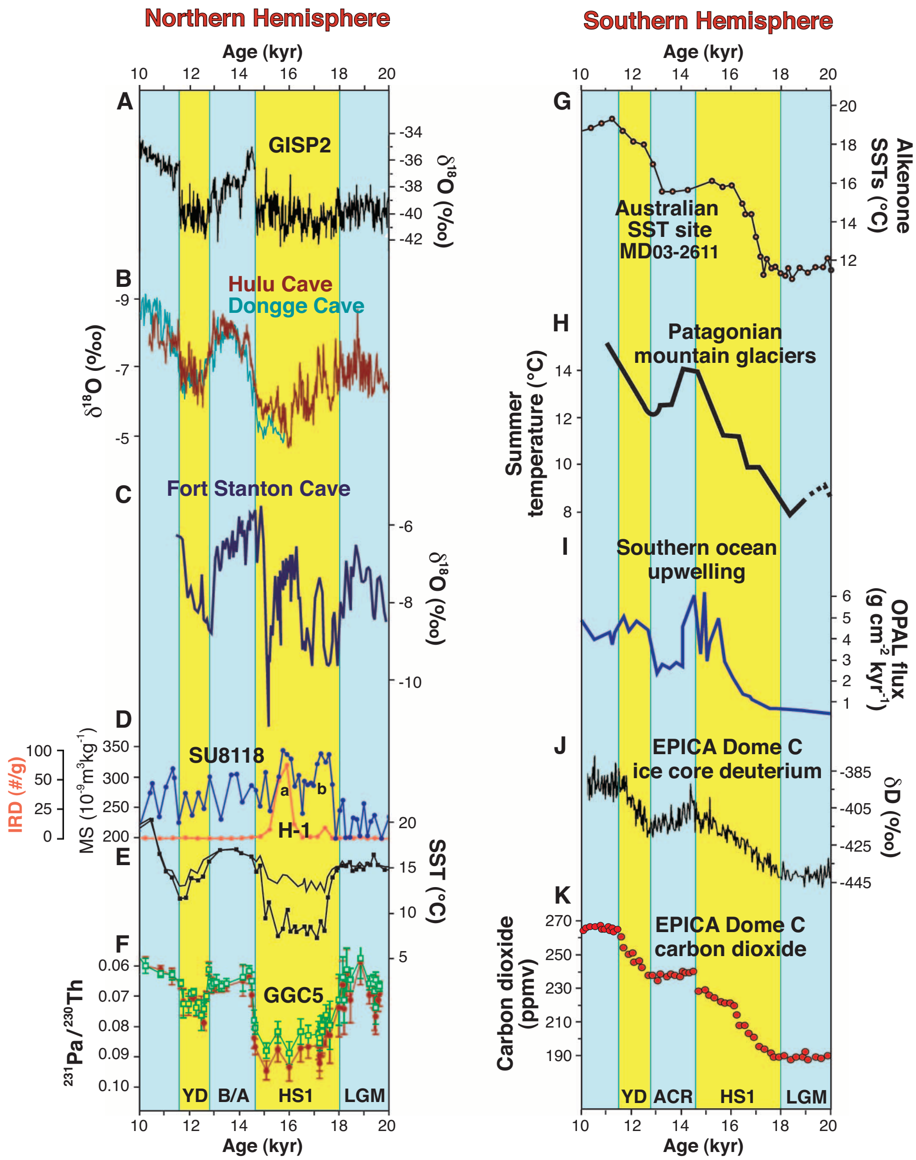


**Fig. 3.** (**A**) Greenland Ice Sheet Project 2 (GISP2) oxygen isotopes (*66*). (**B**) Chinese monsoon records reconstructed from speleothems [drier is down, wetter up (*67*, *68*)]. (**C**) Precipitation record reconstructed from Fort Stanton Cave, southwestern United States [wetter down, drier up (*69*)]. (**D**) Magnetic susceptibility (MS) and ice-rafted detritus (IRD) from marine sediments located off the coast of Portugal (*19*), where IRD is expressed as the number of grains per gram for the size fraction greater than 150 μm. H-1 is Heinrich Event 1. (**E**) SST based on alkenone unsaturated ratios from North Atlantic marine sediment core SU-8118 (*19*). (**F**) The $^{231}Pa/^{230}Th$ ratios from core GGC5 off the Bermuda Rise, where increasing values (plotted downward) reflect reduced Atlantic overturning circulation (*70*). (**G**) SST from a site south of Australia (36°44′S; 136°3′E) reconstructed by using the alkenone unsaturation index (*37*). (**H**) Summer temperature changes determined from glacier and vegetation fluctuations in the Andes of Patagonia in southern South America (*35*, *71*). (**I**) Biogenic opal flux in the Southern Ocean, interpreted as a proxy for changes in upwelling south of the Antarctic Polar Front (*43*). (**J**) European Project for Ice Coring in Antarctica (EPICA) Dome C (EDC) deuterium record (*72*) as a proxy for temperature in Antarctica. (**K**) EDC $CO_2$ record (*72*). EPICA deuterium and $CO_2$ data are plotted on the GISP2 time scale [after (*73*)]. Heinrich stadial 1 (HS1) and the Younger Dryas stadial (YD) are marked with yellow backgrounds, whereas the Bølling-Allerød (B/A), which is contemporary with the Antarctic Cold Reversal (ACR), and LGM have blue backgrounds.

warming of mean annual temperatures (Fig. 3E). The Asian monsoon strengthened (Fig. 3B), and the ITCZ shifted northward. In the south, the termination stalled during the ACR.

There are at least two ways to explain this opposing behavior between the hemispheres. One invokes the oceanic bipolar seesaw by which weakening North Atlantic overturning during HS1 and the YDS reduced northward ocean heat transport (*41*), thereby warming the SH. In addition, reduced North Atlantic overturning would have stimulated deepwater formation in the Southern Ocean, further warming the Southern Ocean and Antarctica during NH stadials (*42*).

A second and complementary mechanism involves a southward shift of the southern westerly wind belt each time the ITCZ was pushed toward the SH by the spread of winter sea ice over the northern North Atlantic (*43*). Such a mechanism would have the advantage of transferring the effects of northern millennial-scale stadial/interstadial events rapidly into the SH. The two processes likely acted synergistically. For example, the bipolar seesaw facilitated the southward shift of the zonal wind systems by changing SST gradients (*44*).

Climate-related shifts in the mean position of the SH westerlies are supported by a number of independent lines of evidence. For example, the latitude of maximum precipitation along the west coast of South America, which coincides with storm tracks that follow the westerlies, was located several degrees north of its present position during the LGM (*45*). Also, during the LGM the SH oceanic Subtropical Front (STF) was situated north of its present position, a condition that has been linked to a northward displacement of the westerlies (*36*, *46*). In contrast to the LGM, a displacement of the SH westerlies to an extreme southerly latitude during terminations is inferred by tracking the STF (*36*) and from estimates of the volume of Agulhas Current water transported into the South Atlantic Ocean, which is controlled by the distance of the STF from the southern tip of Africa (*46*, *47*).

Southward movement of the STF was a contributing factor for the large amplitude and rapid rise of temperatures during HS1 and the YDS within the region between 35°S and 45°S (Fig. 3, G and H) (*17*, *36*–*38*, *40*). This latitude zone also contains the mountain glaciers that began retreating rapidly at ~18 thousand years ago (ka) (*35*). Rapidly warming ocean temperatures "upwind" of the temperate mountain glaciers provided a heat source to stimulate glacier retreat (*38*).

A southward displacement of the SH westerlies during NH stadials would have warmed the Southern Ocean and Antarctica by several mechanisms. A southerly position of the winds would have dissipated sea ice more effectively via northward Ekman transport (*48*), thereby exposing the atmosphere to warmer ocean water. Increased wind-driven upwelling south of the Antarctic Polar Front (Fig. 3I) would have further reduced sea ice cover by bringing to the surface deepwater that was warm enough, although still quite cold, to melt sea ice. A southerly position and increased intensity of the westerlies would have warmed the Southern Ocean and Antarctica by increased southward eddy transport of heat (*49*). Lastly, $CO_2$ released by increased upwelling would have warmed the SH along with the rest of Earth.

Thus, we speculate that during HS1 and the YDS, cold conditions in northern winters forced the ITCZ southward, strengthening the NH Hadley cell to transport heat more effectively from the tropics to high northern latitudes (*50*). The SH Hadley cell, by contrast, would have been weakened (*50*), as would the subtropical jet (STJ) that forms at the poleward boundary of the Hadley Cell at high altitudes. Weakening of the southern STJ would have allowed more momentum to be transferred by eddies to the SH subpolar jet (*51*), which, because of its barotropic nature, would have strengthened the surface SH westerlies, forcing the changes in the ocean described above.

## Essential Elements of a Termination

We now return to the role of large NH ice sheets and summer insolation in the last termination. We first note that the size of the Antarctic Ice Sheet changed little. Most of the minor change was concentrated in the Weddell and Ross embayments, where recession was too late to have had a major effect on the termination (*52*). In the north, recession of the Laurentide and Scandinavian ice sheets was underway at least by 20 ka, as sea level started to rise and as meltwater from European ice sheets and mountain glaciers began to enter the Bay of Biscay (*3*). Presumably this recession was in response to an increase in summer insolation that caused ablation zones to enlarge, intensify, and migrate northward. At the same time, North Atlantic SST remained high and may even have been warming before HS1 (*19*). A critical transition occurred about 18 ka when a combination of ice-sheet melting and surging initiated HS1. At that time, ablation became sufficiently intense and widespread to produce a strong meltwater pulse through the Channel River into the North Atlantic. Shortly thereafter, the continued rise of surface ablation, probably accompanied by basal melting of buttressing ice tongues, triggered surges of ice streams along with massive calving of all marine ice margins. The result was unstable collapse of Laurentide, Greenland, and European ice into the North Atlantic (Fig. 1). It seems reasonable to suggest that ice collapse during HS1 was the longest-lived of the last glacial cycle simply because northern ice sheets were then at or near their largest extent and volume. As a result, isostatic depression was presumably greatest, and therefore the conditions for the operation of marine instability mechanisms (SOM) were likely in place.

Heinrich stadials before the last termination induced changes in the SH similar to those of HS1. For example, they were accompanied by warming in Antarctica and a concomitant rise in atmospheric $CO_2$ (*53*), by increased upwelling in the Southern Ocean (*43*), and by increased SST in the vicinity of the STF (*38*, *39*). However, those events did not lead to terminations. Previous studies have suggested that terminations did not materialize at those times because Earth's climate system failed to pass a critical threshold (*17*, *40*, *54*). We propose that this threshold involves the two essential elements mentioned above: rising NH summer insolation and large NH ice sheets prone to instabilities. The key factor is that delivery of freshwater to the North Atlantic, which is required to maintain stadial conditions (*13*) and a southward displacement of the SH westerlies, must have persisted for a sufficient duration to raise atmospheric $CO_2$ above a minimum level necessary to maintain warm conditions globally.

In support of this threshold concept, we note that each of the last four terminations involved extended northern stadial conditions, as indicated by reduced Asian monsoon intensity (*7*). At each termination, the total duration of stadial conditions, excluding brief reversals, was ~5000 years, much greater than for other stadials

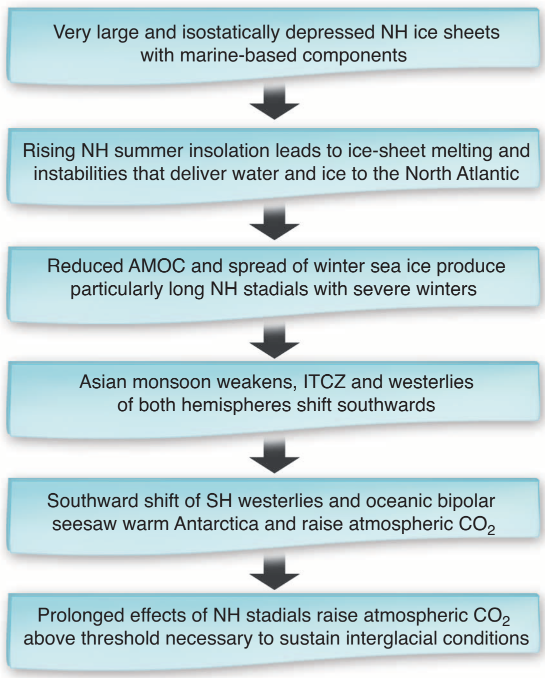


**Fig. 4.** Essential elements of a termination. Summary of the conditions and processes described in the text that contribute to the termination of a Late Pleistocene ice age (e.g., T1 to T4 in Fig. 2). AMOC indicates Atlantic Meridional Overturning Circulation.

evident in the Asian monsoon record (*7*). We attribute this long duration of stadials at terminations to the presence of exceptionally large NH ice sheets, poised for unstable collapse, at the time of increasing NH summer insolation. In this sense, HS1 nearly brought Earth to this threshold, but the YDS was necessary to complete the termination by raising $CO_2$ above the level required to achieve interglacial conditions.

## Broader Implications

Explaining the near coincidence of the last termination in both polar hemispheres has been a long-standing problem. For example, following Milankovitch's (*5*) reasoning that glaciers at middle to high latitudes wax and wane in response to varying summer insolation, Mercer (*55*) noted that recession of middle-latitude SH mountain glaciers during the last termination, that is, a period of declining local summer insolation intensity from the precession effect (18 to 11 ka), "defies explanation." Broecker (*56*) suggested that changes in atmospheric $CO_2$ would help resolve this problem by synchronizing the hemispheres, but he could not identify a mechanism that would cause $CO_2$ to change before NH ice volume.

Our hypothesis addresses this dilemma of coupling the hemispheres during the last termination despite out-of-phase summer insolation signals. We suggest that the combined influence of the oceanic bipolar seesaw and the southward displacement of the SH westerlies, both linked to northern stadials, allowed the high southern latitudes to warm as a result of melting and collapse of NH ice sheets into the North Atlantic. Invoking the same principles, we suggest that a northward displacement of the ITCZ and of the SH westerlies at the onset of the Bølling (~14.7 ka) created the pause in the warming of Antarctica midway through the last termination.

Our hypothesis further points to higher atmospheric $CO_2$, driven by the reorganization of ocean and atmospheric circulation that accompanied northern stadials, as a key factor to complete the deglaciation (Fig. 4). Specifically, it was the long duration of stadial conditions made possible by large and unstable ice sheets that extracted enough $CO_2$ from the deep ocean to warm Earth and then to sustain melting of NH ice sheets for several thousand years after NH summer insolation started to decline. We suggest that this combination of factors was instrumental in terminating the last ice age on a global scale. Furthermore, the effects of these long northern stadials could well have been augmented by the consequences of orbitally induced lengthening of summers and shortening of winters in high southern latitudes (*57*).

Our hypothesis also implies widespread reorganizations of atmospheric circulation during the last termination. Changes in the Asian monsoon (Fig. 3B) and in records from lakes [e.g., (*58*)] and speleothems (Fig. 3C) indicate a reorganization of NH winds during North Atlantic stadial periods. Global reorganization of atmospheric circulation forced by such stadial conditions affords a unifying hypothesis for many features of climate variability throughout the last glacial cycle. In addition to explaining key aspects of the last termination, noted above, it provides a mechanism to account for other climate-related signals that have been correlated with stadial-interstadial cycles in Greenland ice cores, such as changes in marine biological productivity and in the intensity of oxygen minimum zones both in the Arabian Sea [e.g., (*59*)] and in the eastern North Pacific [e.g., (*60*)]. It also affords a benchmark for testing and improving climate models, for example, in simulating the response of atmospheric circulation to meridional surface temperature gradients (SOM).

### References and Notes


1. W. S. Broecker, J. van Donk, *Rev. Geophys. Space Phys.* **8**, 169 (1970).
2. G. H. Denton, T. J. Hughes, *The Last Great Ice Sheet* (Wiley Interscience, NY, 1981).
3. S. Toucanne *et al.*, *Quat. Sci. Rev.* **28**, 1238 (2009).
4. A. S. Dyke, V. K. Prest, *Geogr. Phys. Quat.* **41**, 237 (1987).
5. M. Milankovitch, *Kanon der Erdbestrahlung und Seine Andwendung auf das Eiszeitenproblem* (Royal Serbian Academy Special Publication 132, Belgrade, Serbia, 1941).
6. G. Roe, *Geophys. Res. Lett.* **33**, L24703 (2006).
7. H. Cheng *et al.*, *Science* **326**, 248 (2009).
8. K. Kawamura *et al.*, *Nature* **448**, 912 (2007).
9. L. E. Lisiecki, M. E. Raymo, *Paleoceanography* **20**, PA1003 (2005).
10. M. E. Raymo, *Paleoceanography* **12**, 577 (1997).
11. G. H. Denton, T. J. Hughes, *Quat. Sci. Rev.* **21**, 193 (2002).
12. R. Knutti, J. Flückiger, T. F. Stocker, A. Timmermann, *Nature* **430**, 851 (2004).
13. Z. Liu *et al.*, *Science* **325**, 310 (2009).
14. H. Heinrich, *Quat. Res.* **29**, 142 (1988).
15. G. C. Bond, R. Lotti, *Science* **267**, 1005 (1995).
16. F. Naughton *et al.*, *Earth Planet. Sci. Lett.* **284**, 329 (2009).
17. S. Barker *et al.*, *Nature* **457**, 1097 (2009).
18. G. H. Denton, W. S. Broecker, R. B. Alley, *PAGES News* **14**, 14 (2006).
19. E. Bard, F. Rostek, J.-L. Turon, S. Gendreau, *Science* **289**, 1321 (2000).
20. G. H. Denton, R. B. Alley, G. C. Comer, W. S. Broecker, *Quat. Sci. Rev.* **24**, 1159 (2005).
21. R. F. B. Isarin, H. Renssen, *Earth Sci. Rev.* **48**, 1 (1999).
22. R. F. B. Isarin, H. Renssen, J. Vandenberghe, *J. Quat. Sci.* **13**, 447 (1998).
23. H. Renssen, R. F. B. Isarin, *Global Planet. Change* **30**, 117 (2001).
24. J. C. H. Chiang, C. M. Bitz, *Clim. Dyn.* **25**, 477 (2005).
25. J. P. Severinghaus, T. Sowers, E. J. Brook, R. B. Alley, M. L. Bender, *Nature* **391**, 141 (1998).
26. H. W. Arz, J. Patzold, G. Wefer, *Quat. Res.* **50**, 157 (1998).
27. L. C. Peterson, G. H. Haug, K. A. Hughen, U. Röhl, *Science* **290**, 1947 (2000).
28. G. Leduc, L. Vidal, K. Tachikawa, E. Bard, *Quat. Res.* **72**, 123 (2009).
29. R. Saikku, L. Stott, R. Thunell, *Quat. Sci. Rev.* **28**, 2374 (2009).
30. X. F. Wang *et al.*, *Nature* **432**, 740 (2004).
31. M. L. Griffiths *et al.*, *Nat. Geosci.* **2**, 636 (2009).
32. J. Muller *et al.*, *Quat. Sci. Rev.* **27**, 468 (2008).
33. T. P. Barnett, L. Dümenil, U. Schlese, E. Roeckner, *Science* **239**, 504 (1988).
34. F. Gasse, F. Chalie, A. Vincens, M. A. J. Williams, D. Williamson, *Quat. Sci. Rev.* **27**, 2316 (2008).
35. G. H. Denton *et al.*, *Geogr. Ann. Ser. A* **81A**, 107 (1999).
36. E. L. Sikes *et al.*, *Paleoceanography* **24**, PA2201 (2009).
37. E. Calvo, C. Pelejero, P. De Deckker, G. A. Logan, *Geophys. Res. Lett.* **34**, L13707 (2007).
38. T. T. Barrows, S. Juggins, P. De Deckker, E. Calvo, C. Pelejero, *Paleoceanography* **22**, PA2215 (2007).
39. J. Kaiser, F. Lamy, D. Hebbeln, *Paleoceanography* **20**, PA4009 (2005).
40. F. Lamy *et al.*, *Earth Planet. Sci. Lett.* **259**, 400 (2007).
41. T. J. Crowley, *Paleoceanography* **7**, 489 (1992).
42. W. S. Broecker, *Paleoceanography* **13**, 119 (1998).
43. R. F. Anderson *et al.*, *Science* **323**, 1443 (2009).
44. J. C. H. Chiang, *Annu. Rev. Earth Planet. Sci.* **37**, 263 (2009).
45. P. I. Moreno, T. V. Lowell, G. L. Jacobson Jr., G. H. Denton, *Geogr. Ann. Ser. A* **81A**, 285 (1999).
46. E. Bard, R. E. M. Rickaby, *Nature* **460**, 380 (2009).
47. F. J. C. Peeters *et al.*, *Nature* **430**, 661 (2004).
48. A. Levermann, J. Schewe, M. Montoya, *Geophys. Res. Lett.* **34**, L12711 (2007).
49. J. A. Screen, N. P. Gillett, D. P. Stevens, G. J. Marshall, H. K. Roscoe, *J. Clim.* **22**, 806 (2009).
50. R. S. Lindzen, A. Y. Hou, *J. Atmos. Sci.* **45**, 2416 (1988).
51. S. Lee, H. K. Kim, *J. Atmos. Sci.* **60**, 1490 (2003).
52. H. Conway, B. L. Hall, G. H. Denton, A. M. Gades, E. D. Waddington, *Science* **286**, 280 (1999).
53. J. Ahn, E. J. Brook, *Science* **322**, 83 (2008); published online 11 September 2008 (10.1126/science.1160832).
54. E. W. Wolff, H. Fischer, R. Rothlisberger, *Nat. Geosci.* **2**, 206 (2009).
55. J. H. Mercer, in *Climate Processes and Climate Sensitivity*, J. E. Hansen, T. Takahashi, Eds. (American Geophysical Union, Washington, DC, 1984), pp. 307–313.
56. W. S. Broecker, *Prog. Oceanogr.* **11**, 151 (1982).
57. P. Huybers, G. Denton, *Nat. Geosci.* **1**, 787 (2008).
58. L. Benson, M. Kashgarian, M. Rubin, *Palaeogeogr. Palaeoclimatol. Palaeoecol.* **117**, 1 (1995).
59. M. A. Altabet, M. J. Higginson, D. W. Murray, *Nature* **415**, 159 (2002).
60. J. D. Ortiz *et al.*, *Geology* **32**, 521 (2004).
61. W. S. Broecker, G. H. Denton, *Sci. Am.* **262**, 48 (1990).
62. J. I. Svendsen *et al.*, *Quat. Sci. Rev.* **23**, 1229 (2004).
63. R. Gersonde, X. Crosta, A. Abelmann, L. Armand, *Quat. Sci. Rev.* **24**, 869 (2005).
64. W. G. Thompson, S. L. Goldstein, *Quat. Sci. Rev.* **25**, 3207 (2006).
65. A. Berger, M. F. Loutre, *Quat. Sci. Rev.* **10**, 297 (1991).
66. M. Stuiver, P. M. Grootes, *Quat. Res.* **53**, 277 (2000).
67. Y. J. Wang *et al.*, *Science* **294**, 2345 (2001).
68. D. X. Yuan *et al.*, *Science* **304**, 575 (2004).
69. Y. Asmerom, V. Polyak, S. J. Burns, *Nat. Geosci.* **3**, 114 (2010).
70. J. F. McManus, R. Francois, J. M. Gherardi, L. D. Keigwin, S. Brown-Leger, *Nature* **428**, 834 (2004).
71. J. Strelin, G. H. Denton, *Proceedings of the XVI Congreso Geologico Argentino*, Asociación Geológica Argentina, La Plata, Argentina, 20 to 23 September 2005, article 269.
72. E. Monnin *et al.*, *Science* **291**, 112 (2001).
73. T. M. Marchitto, S. J. Lehman, J. D. Ortiz, J. Flückiger, A. van Geen, *Science* **316**, 1456 (2007).


74. Comments from W. S. Broecker and three anonymous reviewers improved this manuscript. S. Birkel assisted in drafting the figures. Work described in this paper was funded by a grants/cooperative agreement from the National Oceanic and Atmospheric Administration and by the Gary C. Comer Science and Education Foundation. The views expressed herein are those of the authors and do not necessarily reflect the views of NOAA or any of its subagencies. This is Lamont-Doherty Earth Observatory contribution number 7368.


### Supporting Online Material

www.sciencemag.org/cgi/content/full/328/5986/1652/DC1
SOM Text
References

10.1126/science.1184119